



Investigation of the optical properties of MoS₂ thin films using spectroscopic ellipsometry

Chanyoung Yim, Maria O'Brien, Niall McEvoy, Sinéad Winters, Inam Mirza, James G. Lunney, and Georg S. Duesberg

Citation: *Applied Physics Letters* **104**, 103114 (2014); doi: 10.1063/1.4868108

View online: <http://dx.doi.org/10.1063/1.4868108>

View Table of Contents: <http://scitation.aip.org/content/aip/journal/apl/104/10?ver=pdfcov>

Published by the [AIP Publishing](#)

Articles you may be interested in

[Optical properties and phase change transition in Ge₂Sb₂Te₅ flash evaporated thin films studied by temperature dependent spectroscopic ellipsometry](#)

J. Appl. Phys. **104**, 043523 (2008); 10.1063/1.2970069

[Optical properties of amorphous GaAs_{1-x}N_x film sputtering with different N₂ partial pressures](#)

J. Vac. Sci. Technol. A **24**, 1714 (2006); 10.1116/1.2217977

[Effect of metal-ion doping on the optical properties of nanocrystalline ZnO thin films](#)

J. Appl. Phys. **99**, 014306 (2006); 10.1063/1.2158503

[Anisotropic optical properties and molecular orientation in vacuum-deposited ter\(9,9-diarylfuorene\)s thin films using spectroscopic ellipsometry](#)

J. Appl. Phys. **95**, 881 (2004); 10.1063/1.1635991

[Optical characterization of CuIn_{1-x}Ga_xSe₂ alloy thin films by spectroscopic ellipsometry](#)

J. Appl. Phys. **94**, 879 (2003); 10.1063/1.1581345

The logo for AIP Chaos is displayed in white text on a red background. The letters 'AIP' are large and bold, followed by a vertical bar and the word 'Chaos' in a smaller font.

AIP | Chaos

CALL FOR APPLICANTS

Seeking new Editor-in-Chief

Investigation of the optical properties of MoS₂ thin films using spectroscopic ellipsometry

Chanyoung Yim,^{1,2} Maria O'Brien,^{1,2} Niall McEvoy,² Sinéad Winters,^{1,2} Inam Mirza,^{2,3} James G. Lunney,^{2,3} and Georg S. Duesberg^{1,2,4,a)}

¹School of Chemistry, Trinity College Dublin, Dublin 2, Ireland

²Centre for Research on Adaptive Nanostructures and Nanodevices (CRANN), Trinity College Dublin, Dublin 2, Ireland

³School of Physics, Trinity College Dublin, Dublin 2, Ireland

⁴Advanced Materials and BioEngineering Research (AMBER) Centre, Trinity College Dublin, Dublin 2, Ireland

(Received 9 January 2014; accepted 26 February 2014; published online 14 March 2014)

Spectroscopic ellipsometry (SE) characterization of layered transition metal dichalcogenide (TMD) thin films grown by vapor phase sulfurization is reported. By developing an optical dispersion model, the extinction coefficient and refractive index, as well as the thickness of molybdenum disulfide (MoS₂) films, were extracted. In addition, the optical band gap was obtained from SE and showed a clear dependence on the MoS₂ film thickness, with thinner films having a larger band gap energy. These results are consistent with theory and observations made on MoS₂ flakes prepared by exfoliation, showing the viability of vapor phase derived TMDs for optical applications. © 2014 AIP Publishing LLC. [<http://dx.doi.org/10.1063/1.4868108>]

In recent years, there has been a large volume of research conducted on two dimensional (2D) materials such as graphene and transition metal dichalcogenides (TMDs) due to their suitability for future electronic/optoelectronic device applications.^{1–4} In particular, molybdenum disulfide (MoS₂), a semiconducting layered TMD, has been identified as one of the most promising 2D materials for nano-electronic applications because of its properties which can be tuned by controlling the number of layers or by careful selection of substrate/gate dielectric materials.^{5–8} Moreover, unlike pristine graphene which has no band gap, monolayer MoS₂ has a direct band gap of ~1.8 eV and bulk MoS₂ has an indirect band gap of ~1.3 eV,⁵ and electronic devices based on mono- or multilayered MoS₂ films have shown good photodetection capability.^{7,9} While mechanical exfoliation is a widely used method to prepare layered MoS₂ thin films, the difficulty of controlling layer thickness and the lateral size limitation have led to the development of alternative synthesis routes. Recently, vapor-phase growth methods, whereby sulfur powder is vaporized and reacted with thin molybdenum or molybdenum oxide seed layers, have been introduced.^{10–12} This makes it possible to obtain large-area MoS₂ thin films with tunable thickness and such films have been employed to fabricate various types of nano-optoelectronic devices including solar cells, sensors, and phototransistors.^{13–15}

For optoelectronic device applications of MoS₂ to be fully understood, it is necessary to know the refractive index (n) and the extinction coefficient (k). Spectroscopic ellipsometry (SE) is a powerful non-destructive technique to measure the optical properties of thin films. In SE, the wavelength dependent optical constants and the thickness of thin films can be determined by analyzing the change in the polarization state of the reflected light from the film surface and developing an optical dispersion model of the film

material.¹⁶ It is frequently used in industry for film characterization and in *in-situ* thickness monitoring because it is fast, cheap, and non-destructive. In recent years, SE has been employed to investigate the optical constants of graphene;^{17–20} however, to date, SE characterization of 2D layered TMDs, such as MoS₂, has rarely been reported.

In this work, we report the measurement of the optical properties of MoS₂ thin films with different thicknesses using SE. The MoS₂ thin films were synthesized on substrates using a vapor phase sulfurization process and characterized by UV-visible absorption spectroscopy and Raman spectroscopy. Based on SE measurements, an optical dispersion model was developed for the MoS₂ thin films, and the optical constants (n , k) and the film thickness values were extracted. In addition, optical band gap values of the MoS₂ thin films were obtained from analysis of the k values. The values are consistent with data derived from other techniques and theoretical values. This work establishes SE as a viable tool for the characterization of TMDs. Further, our study shows that vapor phase derived MoS₂ exhibits similar optical properties to exfoliated materials, making it a strong candidate for the manufacture for optoelectronic devices.

Vapor phase sulfurization was employed to synthesize MoS₂ thin films, as described in the previous work.^{11,14} Mo (99.99%, MaTecK) films with various thicknesses (1–20 nm) were deposited by sputtering on fused quartz substrates (~10 mm × 10 mm) and on commercially available silicon dioxide (SiO₂, ~290 nm thick) substrates (~10 mm × 10 mm), which were thermally grown on top of <100> oriented crystalline silicon (Si) wafers, using a Gatan Precision Etching and Coating System (PECS). A quartz crystal microbalance was used to monitor the Mo film deposition rate (<0.1 nm/s) and thickness. The Mo samples were sulfurized in a quartz tube furnace consisting of two different heating zones as shown in Figure 1(a). The samples were loaded into the hot zone which was heated to 750 °C and annealed for 30 min at a pressure of

^{a)}Electronic mail: duesberg@tcd.ie

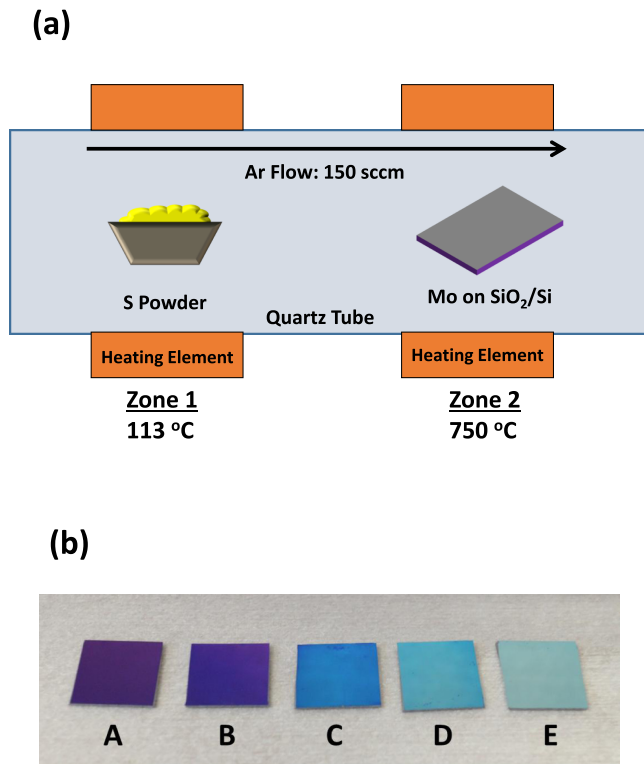


FIG. 1. (a) Schematic diagram of the vapor phase sulfurization process used for MoS₂ thin film synthesis. (b) Photograph of MoS₂ samples with increasing thickness (A–E).

~1 Torr with an argon (Ar) flow of 150 sccm (standard cubic centimeters per minute). Sulfur vapor was then produced by heating sulfur powder (MaTecK, 99%) up to its melting point (~113 °C) in the second upstream heating zone of the furnace and transported to the Mo samples using Ar gas as carrier. After sulfurization, the samples were annealed for 30 min at 750 °C and then cooled down to room temperature. Raman spectroscopy measurements were carried out with a HORIBA Jobin-Yvon Labram HR, using an excitation wavelength of 532 nm and an 1800 lines/mm grating. UV-visible absorption

data were obtained with a Varian Cary 6000i double beam spectrophotometer in the spectral range of 200–800 nm. The SE characterization of the MoS₂ thin films was conducted using an Alpha SE tool (J. A. Woollam Co., Inc.) operating in the wavelength range of 380–900 nm (1.38–3.26 eV) at an angle of incidence of 70° with a beam spot size of ~40 mm² and a rotating compensator. SE data were analyzed using CompleteEASE 4.72 (J. A. Woollam Co., Inc.). X-ray reflectivity (XRR) measurements were conducted using a Bruker D8-Discover X-ray diffractometer which is fitted with Cu K-alpha X-ray source and Goebel mirror to produce a parallel beam. Thickness values were obtained by fitting the XRR data using a computer simulation called LEPTOS.

In our synthesis, vaporized sulfur reacts with pre-deposited Mo layers, yielding continuous MoS₂ thin films. An optical image of MoS₂ thin films on SiO₂/Si substrates (samples A, B, C, D, and E) is shown in Figure 1(b). The samples are clearly distinguishable from each other due to the surface color difference caused by their varying thicknesses. The films appear homogeneous over the sample area of ~10 mm × 10 mm.

The optical properties of the MoS₂ thin films were measured by SE. The raw SE data comprise a tabulation versus wavelength of the amplitude ratio (Ψ , psi) and the phase difference (Δ , delta) between the p- and s-polarized components of the reflected light. The two parameters measured by a SE system are related to the ratio ρ , defined by the equation of $\rho = r_p/r_s = \tan(\Psi)\exp(i\Delta)$, where r_p and r_s are the amplitude reflection coefficients for the p-polarized and s-polarized light, respectively.¹⁶ A four-layer optical model which consists of a Si substrate, an interface layer between Si and SiO₂, a SiO₂ layer, and a MoS₂ layer was built to analyze the SE spectra. Each layer of the model has several fitting variables such as thickness and optical dispersion model parameters. A value of the goodness of fit, which quantifies how well the data generated by the optical model (G) fit the experimental data (E), is derived from the root mean squared error (MSE) as defined by

$$MSE = \sqrt{\frac{1}{3m-l} \sum_{i=1}^m [(N_{E_i} - N_{G_i})^2 + (C_{E_i} - C_{G_i})^2 + (S_{E_i} - S_{G_i})^2]} \times 1000, \quad (1)$$

where m is the number of wavelengths measured, l is the number of fit parameters, and $N = \cos(2\Psi)$, $C = \sin(2\Psi)\cos(\Delta)$, $S = \sin(2\Psi)\sin(\Delta)$.²¹ The Levenberg-Marquardt nonlinear regression algorithm is used to minimize the MSE during the fitting process.

In a multilayer structure model, it is important to define the optical response of underlying layers in order to minimize optical correlation effects between layers and find more accurate values for the optical constants and the thickness of the top layer. Therefore, SE spectra of reference SiO₂/Si substrates, where Mo layers were not deposited, were first measured and analyzed using a three-layer optical

model composed of a Si substrate, an interface layer between Si and SiO₂, and a SiO₂ layer. It is assumed that the underlying layers are stable with well-established optical constants.²² The crystalline Si substrate of the model can be presumed to have a semi-infinite thickness, so the thicknesses of the interface and SiO₂ layers were determined from the fitting process. Then, the MoS₂ layer is added on top of the SiO₂ layer in the model structure, allowing its optical properties to be characterized in the presence of well-defined underlying layers. A Tauc-Lorentz (T-L) oscillation model was used to determine the optical properties of the MoS₂ thin film. The complex dielectric function of the energy (E)

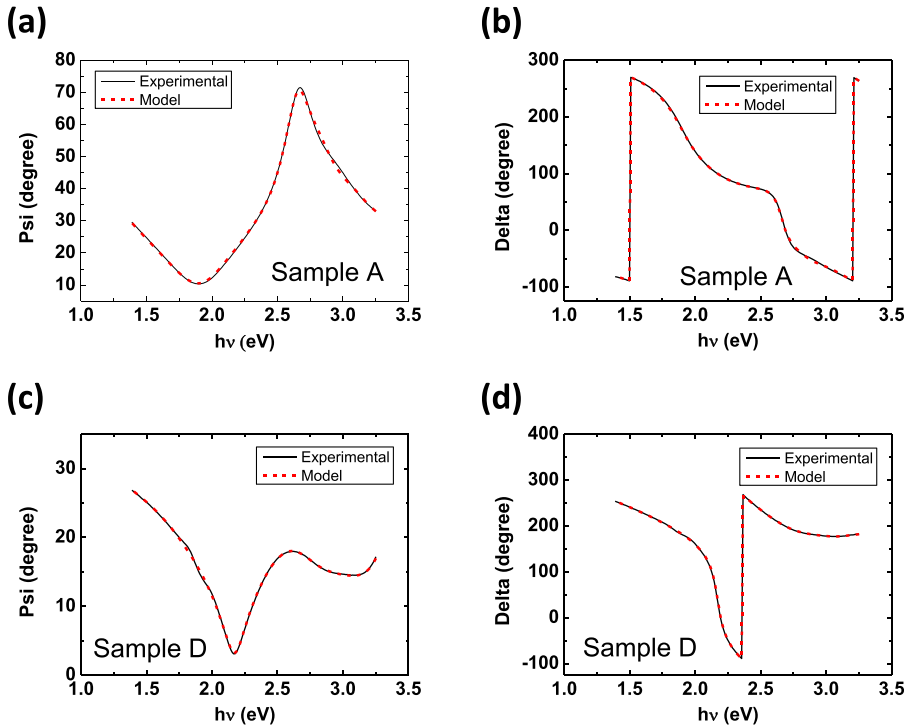


FIG. 2. Plots of the experimental and simulated (model) SE spectra (psi and delta) of MoS₂ samples A and D: (a) Ψ and (b) Δ data of sample A, and (c) Ψ and (d) Δ data of sample D.

is defined as $\varepsilon(E) = \varepsilon_1 + i\varepsilon_2$. In the T-L model, ε_1 and ε_2 are defined as

$$\varepsilon_2 = \left[\frac{AE_0C(E - E_b)^2}{(E^2 - E_0^2)^2 + C^2E^2} \times \frac{1}{E} \right] \text{ for } E > E_b, \quad (2)$$

$$\varepsilon_2 = 0 \text{ for } E \leq E_b,$$

$$\varepsilon_1 = \varepsilon_1(\infty) + \frac{2}{\pi} P \int_{E_b}^{\infty} \frac{\xi \varepsilon_2(\xi)}{\xi^2 - E^2} d\xi, \quad (3)$$

where A , E_0 , C , and E_b represent the amplitude, center energy, broadening, and band gap of the oscillator, respectively, which all have units of energy (eV), and P stands for the Cauchy principal part of the integral.²³ The thickness of MoS₂ and the fitting parameters of the T-L oscillation model are varied, until the best fit between experimental spectra and simulated data from the optical model is achieved with the lowest MSE values. The experimental and simulated spectra (Ψ and Δ) for MoS₂ samples A and D are depicted in Figure 2, showing a good match between them. Additional spectral data for other samples (B, C, and E) are presented in Figure S1 of the supplementary material.²⁸ Extracted MoS₂ thickness values of the five samples (A, B, C, D, and E) are 1.99 ± 0.01 nm, 3.01 ± 0.07 nm, 5.53 ± 0.08 nm, 9.83 ± 0.04 nm, and 19.88 ± 0.05 nm, respectively. More details on fitting parameter values of the T-L oscillation model for the best fit are listed in

the supplementary material (Table S1).²⁸ In addition, XRR measurements of the samples were conducted to verify the MoS₂ film thickness, and the measured values were consistent with those extracted from SE measurements. The thickness values of the MoS₂ thin films from SE and XRR measurements are summarized in Table I. More details on XRR measurements are presented in the supplementary material.²⁸ Figures 3(a) and 3(b) show n and k values of the MoS₂ layer for each sample derived from the optical model with the best fits. Two dominant peaks are observed at the energy of ~ 2.0 eV and ~ 2.9 eV in the k plot. In addition, an absorbance spectrum of a MoS₂ thin film (~ 20 nm) on a quartz substrate was measured, as shown in the inset of Figure 3(b). Two spectral regions with dominant absorption variations are observed in the photon energy range of 1.5 eV–3.8 eV, which are related to A/B excitonic peaks in the range of 1.8–2.0 eV, and C/D excitonic peaks in the range of 2.7–3.1 eV, respectively.²⁴ This shows good agreement with the two k peaks observed at energies of ~ 2.0 eV and ~ 2.9 eV in the k plot.

Raman spectra were measured from the MoS₂ thin films on the SiO₂/Si substrates. When probed with a 532 nm excitation laser, bulk MoS₂ has two well-known Raman bands at ~ 383 cm⁻¹ and ~ 408 cm⁻¹ which correspond to E_{2g}^1 and A_{1g} vibrational modes, respectively.²⁵ Raman spectra of five films, with different thicknesses, are shown in Figure 4. It is evident that the E_{2g}^1 and A_{1g} peaks shift closer to one another with decreasing film thickness. This is consistent with the

TABLE I. Summary of the MoS₂ thickness values from SE data and XRR measurements for the five MoS₂ samples (samples A, B, C, D, and E). Thickness values of samples A and B from XRR measurements are not available due to the thickness resolution limit of XRR.

	Sample	A	B	C	D	E
SE	Thickness (nm)	1.99 ± 0.01	3.01 ± 0.07	5.53 ± 0.08	9.83 ± 0.04	19.88 ± 0.05
	MSE	4.100	7.067	3.606	4.429	5.173
XRR	Thickness (nm)	N.A.	N.A.	4.4 ± 1.4	9.9 ± 1.6	19.4 ± 1.6

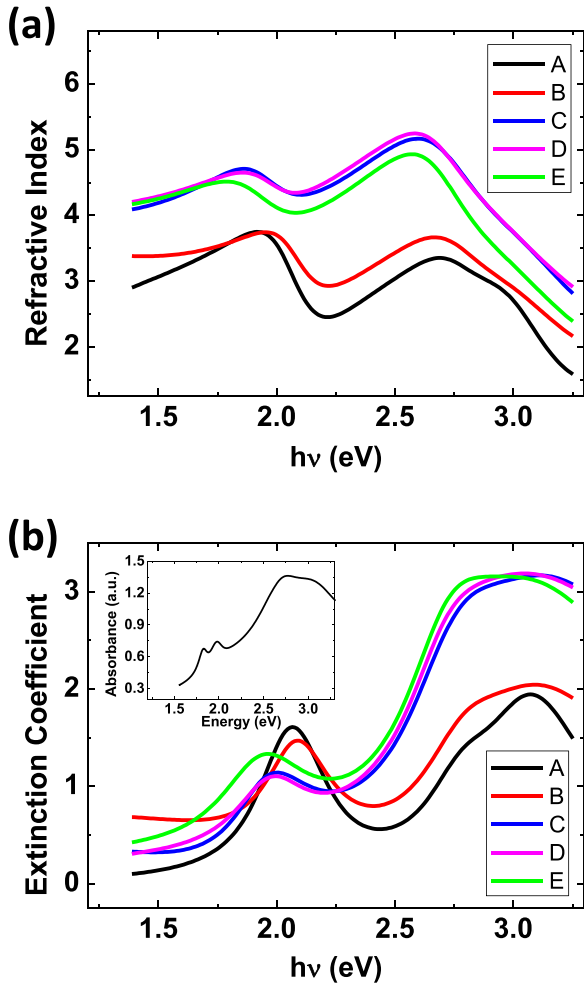


FIG. 3. Plots of (a) the refractive index n and (b) extinction coefficient k values of the MoS₂ layers for the five samples (A, B, C, D and E) derived from the optical model with the best fits. The inset of (b) shows a UV-visible absorption spectrum of a MoS₂ thin film on a quartz substrate.

report of Li *et al.*,²⁵ who described the layer thickness dependence of the Raman signal of mechanically exfoliated MoS₂ with decreasing layer thicknesses. In the case of sample E, the E_{2g}^1 and A_{1g} peaks are seen at 384.2 cm^{-1} and 409.6 cm^{-1} , a separation of 25.4 cm^{-1} , whereas for sample A, the same peaks manifest at 387.0 cm^{-1} and 407.1 cm^{-1} , a separation of 20.1 cm^{-1} . This suggests that sample A

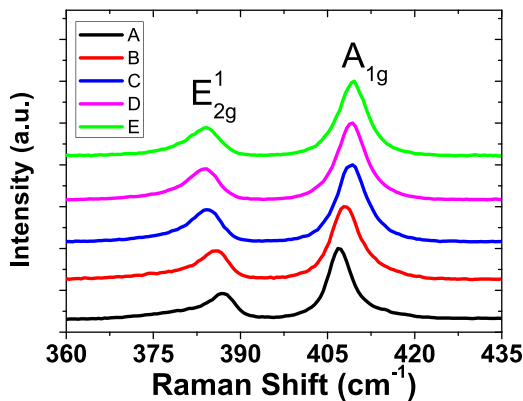


FIG. 4. Raman spectra of the MoS₂ thin films on the SiO₂/Si substrates (samples A, B, C, D, and E).

consists of very few (1–3) layers, whereas sample E behaves like bulk MoS₂.

Furthermore, studies of the optical band gap energy of the MoS₂ thin films were conducted. The optical absorption coefficient (α) of MoS₂ thin films can be calculated from the extinction coefficient k and wavelength λ by means of $\alpha = 4\pi k/\lambda$. The relationship between absorption coefficient α and the photon energy can be expressed by

$$\alpha = \frac{K(h\nu - E_g)^m}{h\nu}, \quad (4)$$

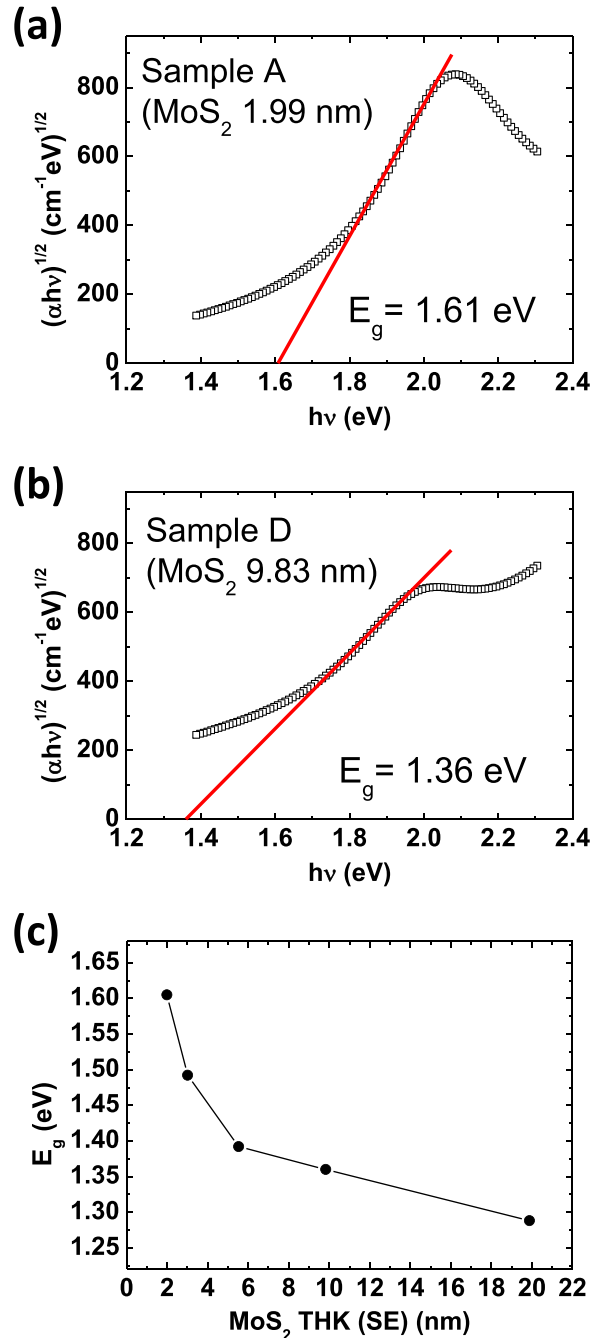


FIG. 5. (a) Plot of $(\alpha h\nu)^{1/2}$ vs. $h\nu$ for sample A. (b) Plot of $(\alpha h\nu)^{1/2}$ vs. $h\nu$ for sample D. The extrapolation of the linear region to $(\alpha h\nu)^{1/2} = 0$ (red line) gives the E_g value. (c) Plot of E_g vs. MoS₂ thickness for samples A, B, C, D, and E.

where K is a constant, $h\nu$ is the incident photon energy, and m is a number that characterizes the transition process.^{26,27} Depending on the transition type, m has a value of 1/2 for direct transition and 2 for indirect transition. Since our MoS₂ thin films are considered as multilayer MoS₂ films with thicknesses of 1.99–19.88 nm, it is believed that they have primarily indirect band gap transitions.⁵ Thus, the variation of α with $h\nu$ can be determined by using the relation of $(\alpha h\nu)^{1/2} \sim (h\nu - E_g)$ and the optical band gap E_g can be extracted by extrapolating the linear region of a $(\alpha h\nu)^{1/2}$ vs. $h\nu$ plot to $(\alpha h\nu)^{1/2} = 0$. Plots of $(\alpha h\nu)^{1/2}$ vs. $h\nu$ for the MoS₂ thin films (samples A and D) are shown in Figures 5(a) and 5(b). The extracted E_g values of the five samples are 1.61, 1.49, 1.45, 1.36, and 1.29 eV for samples A, B, C, D, and E, respectively. Additional plots of $(\alpha h\nu)^{1/2}$ vs. $h\nu$ for samples B, C, and E are shown in Figure S3 of the supplementary material.²⁸ It is evident that the thinner MoS₂ films have a larger E_g , as presented in Figure 5(c). The thinnest MoS₂ film (sample A) with a measured thickness of 1.99 nm shows the largest E_g (1.61 eV), and as the MoS₂ film thickness increases E_g decreases towards the band gap of bulk MoS₂ (~ 1.3 eV). These first ellipsometric measurements of layered MoS₂ films are comparable with the previous reports on E_g of single and multilayer MoS₂ derived by exfoliation. Mak *et al.*⁵ and Lee *et al.*⁷ characterized the optical band gap energy of single and few layer mechanically exfoliated MoS₂ from photoluminescence (PL) spectra and electrical measurements of MoS₂ phototransistors, respectively, and found that the band gap decreased in energy with increasing MoS₂ thickness. Eda *et al.*²⁴ also observed a similar trend in E_g from chemically exfoliated MoS₂ using PL spectra measurements. This consistency is notable, since it implies that our vapor phase derived MoS₂ has comparable optical characteristics to those of exfoliated materials. Our study further establishes SE as a viable tool for the characterization of 2D materials as it can be used to investigate E_g of MoS₂, or indeed other TMDs (e.g., WTe₂, MoSe₂, etc.), while also giving information on optical constants and thicknesses. Such measurements are fast, non-destructive, and relatively easy to perform.

In summary, SE measurements have been carried out on MoS₂ thin films with different thicknesses synthesized by vapor phase sulfurization. In addition, they were characterized by XRR, UV-visible absorption spectroscopy, and Raman spectroscopy. An optical dispersion model of MoS₂ was developed for SE data analysis. Values of optical constants (n , k) and the thickness were determined by fitting the optical model function to the experimental data. The optical band gap energy E_g of the MoS₂ thin films was also investigated. Using the absorption coefficients of MoS₂ calculated from the k values, E_g of each MoS₂ film was extracted. The E_g values of the MoS₂ films show a clear dependence on the

MoS₂ film thickness, indicating that thinner MoS₂ films have a larger E_g . This study establishes SE as a promising technique for optical characterization of TMD films.

This work was supported by the SFI under Contract No. 08/CE/I1432, 12/RC/2278, and PI_10/IN.1/I3030. C.Y. and M.O. acknowledge the Embark Initiative via an Irish Research Council scholarship.

- ¹K. S. Novoselov, D. Jiang, F. Schedin, T. J. Booth, V. V. Khotkevich, S. V. Morozov, and A. K. Geim, *Proc. Natl. Acad. Sci. U.S.A.* **102**, 10451 (2005).
- ²A. H. C. Neto and K. Novoselov, *Mater. Express* **1**, 10 (2011).
- ³K. S. Novoselov, *Rev. Mod. Phys.* **83**, 837 (2011).
- ⁴Q. H. Wang, K. Kalantar-Zadeh, A. Kis, J. N. Coleman, and M. S. Strano, *Nat. Nanotechnol.* **7**, 699 (2012).
- ⁵K. F. Mak, C. Lee, J. Hone, J. Shan, and T. F. Heinz, *Phys. Rev. Lett.* **105**, 136805 (2010).
- ⁶B. Radisavljevic, A. Radenovic, J. Brivio, V. Giacometti, and A. Kis, *Nat. Nanotechnol.* **6**, 147 (2011).
- ⁷H. S. Lee, S.-W. Min, Y.-G. Chang, M. K. Park, T. Nam, H. Kim, J. H. Kim, S. Ryu, and S. Im, *Nano Lett.* **12**, 3695 (2012).
- ⁸B. Radisavljevic and A. Kis, *Nature Mater.* **12**, 815 (2013).
- ⁹O. Lopez-Sanchez, D. Lembke, M. Kayci, A. Radenovic, and A. Kis, *Nat. Nanotechnol.* **8**, 497 (2013).
- ¹⁰Y.-H. Lee, X.-Q. Zhang, W. Zhang, M.-T. Chang, C.-T. Lin, K.-D. Chang, Y.-C. Yu, J. T.-W. Wang, C.-S. Chang, L.-J. Li, and T.-W. Lin, *Adv. Mater.* **24**, 2320 (2012).
- ¹¹Y. Zhan, Z. Liu, S. Najmaei, P. M. Ajayan, and J. Lou, *Small* **8**, 966 (2012).
- ¹²S. Najmaei, Z. Liu, W. Zhou, X. Zou, G. Shi, S. Lei, B. I. Yakobson, J.-C. Idrobo, P. M. Ajayan, and J. Lou, *Nature Mater.* **12**, 754 (2013).
- ¹³M. Shanmugam, C. A. Durcan, and B. Yu, *Nanoscale* **4**, 7399 (2012).
- ¹⁴K. Lee, R. Gatensby, N. McEvoy, T. Hallam, and G. S. Duesberg, *Adv. Mater.* **25**, 6699 (2013).
- ¹⁵W. Zhang, J.-K. Huang, C.-H. Chen, Y.-H. Chang, Y.-J. Cheng, and L.-J. Li, *Adv. Mater.* **25**, 3456 (2013).
- ¹⁶H. Fujiwara, *Spectroscopic Ellipsometry: Principles and Applications* (John Wiley & Sons Ltd, Chichester, 2007), p. 81.
- ¹⁷V. G. Kravets, A. N. Grigorenko, R. R. Nair, P. Blake, S. Anissimova, K. S. Novoselov, and A. K. Geim, *Phys. Rev. B* **81**, 155413 (2010).
- ¹⁸F. J. Nelson, V. K. Kamineni, T. Zhang, E. S. Comfort, J. U. Lee, and A. C. Diebold, *Appl. Phys. Lett.* **97**, 253110 (2010).
- ¹⁹J. W. Weber, V. E. Calado, and M. C. M. van de Sanden, *Appl. Phys. Lett.* **97**, 091904 (2010).
- ²⁰A. Matkovic, U. Ralevic, M. Chhikara, M. M. Jakovljevic, D. Jovanovic, G. Bratina, and R. Gajic, *J. Appl. Phys.* **114**, 093505 (2013).
- ²¹*CompleteEASE™ Data Analysis Manual Version 4.63*, J. A. Woollam Co., Inc., Lincoln, NE, 2011, p. 45.
- ²²C. M. Herzinger, B. Johs, W. A. McGahan, J. A. Woollam, and W. Paulson, *J. Appl. Phys.* **83**, 3323 (1998).
- ²³G. E. Jellison and F. A. Modine, *Appl. Phys. Lett.* **69**, 371 (1996).
- ²⁴G. Eda, H. Yamaguchi, D. Voiry, T. Fujita, M. Chen, and M. Chhowalla, *Nano Lett.* **11**, 5111 (2011).
- ²⁵H. Li, Q. Zhang, C. C. R. Yap, B. K. Tay, T. H. T. Edwin, A. Olivier, and D. Baillargeat, *Adv. Funct. Mater.* **22**, 1385 (2012).
- ²⁶F. P. Koffyberg, K. Dwight, and A. Wold, *Solid State Commun.* **30**, 433 (1979).
- ²⁷E. R. Shaaban, M. S. Abd El-Sadek, M. El-Hagary, and I. S. Yahia, *Phys. Scr.* **86**, 015702 (2012).
- ²⁸See supplementary material at <http://dx.doi.org/10.1063/1.4868108> for additional SE spectral data, fitting parameter values of the T-L oscillation model, XRR details, and plots on the optical band gap extraction.